JACC: CARDIOVASCULAR IMAGING
VOL. 2, NO. 10, 2009

ISSN 1936-878X/09/$36.00
PUBLISHED BY ELSEVIER INC.
DOI:10.1016/j.jcmg.2009.06.013

CVN Interview

Effects of Adenosine and a Selective A_{2A} Adenosine Receptor Agonist on Hemodynamic and Thallium-201 and Technetium-99m–SestaMIBI Biodistribution and Kinetics

Choukri Mekkaoui, PhD,* Farid Jadbabaie, MD,* Donald P. Dione, BS,*
David F. Meoli, MD, PhD,* Kailasnath Purushothaman, PhD,† Luiz Belardinelli, MD,‡
Albert J. Sinusas, MD*†

New Haven, Connecticut; and Palo Alto, California

OBJECTIVES The purpose of this study was to compare a selective A_{2A} adenosine receptor agonist (regadenoson) with adenosine in clinically relevant canine models with regard to effects on hemodynamics and thallium-201 (^{201}Tl) and technetium-99m (^{99m}Tc)-sestaMIBI biodistribution and kinetics.

BACKGROUND The clinical application of vasodilator stress for perfusion imaging requires consideration of the effects of these vasodilating agents on systemic hemodynamics, coronary flow, and radiotracer uptake and clearance kinetics.

METHODS Sequential imaging and arterial blood sampling was performed on control, anesthetized closed-chest canines (n = 7) to evaluate radiotracer biodistribution and kinetics after either a bolus administration of regadenoson (2.5 μg/kg) or 4.5-min infusion of adenosine (280 μg/kg). The effects of regadenoson on coronary flow and myocardial radiotracer uptake were then evaluated in an open-chest canine model of a critical stenosis (n = 7). Results from ex vivo single-photon emission computed tomography were compared with tissue well-counting.

RESULTS The use of regadenoson compared favorably with adenosine in regard to the duration and magnitude of the hemodynamic effects and the effect on ^{201}Tl and ^{99m}Tc-sestaMIBI biodistribution and kinetics. The arterial blood clearance half-time was significantly faster for ^{99m}Tc-sestaMIBI (regadenoson: 1.4 ± 0.03 min; adenosine: 1.5 ± 0.08 min) than for ^{201}Tl (regadenoson: 2.5 ± 0.16 min, $p < 0.01$; adenosine: 2.7 ± 0.04 min, $p < 0.01$) for both vasodilator stressors. The relative microsphere flow deficit (0.34 ± 0.02%) during regadenoson stress was significantly greater than the relative perfusion defect with ^{99m}Tc-sestaMIBI (0.69 ± 0.03%, $p < 0.001$) or ^{201}Tl (0.53 ± 0.02%, $p < 0.001$), although ^{201}Tl tracked the flow deficit within the ischemic region better than ^{99m}Tc-sestaMIBI. The perfusion defect score was larger with ^{201}Tl (22 ± 2.8% left ventricular) than with ^{99m}Tc-sestaMIBI (17 ± 1.7% left ventricular, $p < 0.05$) on ex vivo single-photon emission computed tomography images.

CONCLUSIONS The bolus administration of regadenoson produced a hyperemic response comparable to a standard infusion of adenosine. The biodistribution and clearance of both ^{201}Tl and ^{99m}Tc-sestaMIBI during regadenoson were similar to adenosine vasodilation. Ex vivo perfusion images under the most ideal conditions permitted detection of a critical stenosis, although ^{201}Tl offered significant advantages over ^{99m}Tc-sestaMIBI for perfusion imaging during regadenoson vasodilator stress. (J Am Coll Cardiol Img 2009; 2:1198–208) © 2009 by the American College of Cardiology Foundation

From the *Division of Cardiovascular Medicine, Department of Internal Medicine, and †Department of Diagnostic Radiology, Yale University School of Medicine, New Haven, Connecticut; and ‡CV Therapeutics, Inc., Palo Alto, California. This research was supported in part by a grant-in-aid from the Heritage Affiliate of American Heart Association (to Dr. Purushothaman), Robbinsville, New Jersey, and a grant from CV Therapeutics, Inc. (to Dr. Sinusas).

Manuscript received September 2, 2008; revised manuscript received June 4, 2009, accepted June 10, 2009.

Myocardial stress-rest perfusion imaging is used to detect coronary artery disease. Thallium-201 (^{201}Tl)-labeled and technetium-99m (^{99m}Tc)-labeled tracers, such as ^{99m}Tc-sestaMIBI (^{99m}Tc-MIBI), are used interchangeably for the detection of coronary artery disease. However, there are substantial differences in myocardial uptake, clearance kinetics, and biodistribution among the ^{99m}Tc-labeled tracers and ^{201}Tl (1,2), which should be considered in myocardial perfusion imaging (MPI).

See page 1209

The accuracy of MPI is dependent on the biodistribution of tracers in organs adjacent to the heart (i.e., lungs, liver) and affects the optimal timing of MPI (3). Patients with a critical coronary stenosis who are unable to exercise are injected during pharmacological vasodilator stress to mimic alterations in coronary flow associated with exercise stress. The level or type of stress can affect the biodistribution (4–8). The biodistribution of ^{99m}Tc-MIBI is altered by exercise or pharmacological stress, suggesting that the kinetics also are influenced (3). The uptake of ^{99m}Tc-MIBI plateaus at high flows during adenosine vasodilator stress, potentially underestimating myocardial perfusion defect size (9).

Adenosine used for stress MPI causes systemic vascular and hemodynamic side effects, possibly altering the biodistribution of radiotracers (9). Most adverse effects can be attributed to A_1, A_{2B}, and A_3 adenosine receptor stimulation (10). Selective A_{2A} adenosine receptor agonists may reduce unwanted effects but may alter radiotracer kinetics. Regadenoson (CVT-3146, CV Therapeutics, Inc., a subsidiary of Gilead, Foster City, California), an A_{2A} agonist, is a potent vasodilator with a short duration of action and minimal hemodynamic effects (10,11). Recent clinical trials (12–16) have established regadenoson as a vasodilator for MPI.

Studies in conscious dogs and humans demonstrated that the dose and rate of regadenoson administration affects hemodynamics (11) and coronary flow (10,17,18). Differential effects of regadenoson on renal and splanchnic flow may affect the biodistribution and clearance of radiotracers, having an impact on the efficacy of the vasodilator MPI.

Regadenoson duration of action and differential effects on flow (coronary and systemic) compared with adenosine may result in favorable tracer kinetics for MPI. To determine whether regadenoson results in favorable conditions for vasodilator MPI, we evaluated the uptake, biodistribution, and clearance of ^{201}Tl and ^{99m}Tc-MIBI during vasodilation with regadenoson and adenosine in chronic, closed-chest canine models. To establish the linearity of radiotracer uptake during regadenoson stress, we used acute open-chest canine models with a critical stenosis.

METHODS

Surgical preparation. Fasting adult mongrel dogs (23 ± 0.9 kg) were anesthetized with intravenous sodium thiamylal (20 mg/kg). Animals were intubated and ventilated with a mixture of halothane (0.5% to 1.5%), nitrous oxide and oxygen (N_2O:O_2 = 3:1). An electrocardiogram (ECG) lead was used for heart rate (HR) and rhythm monitoring. The protocol was approved by Yale Institutional Animal Care and Use Committee in compliance with guiding principles of the American Physiologic Society on research animal use.

CHRONIC MODEL. Venous access was established for administration of radiotracer and regadenoson or adenosine. A femoral artery was cannulated for blood sampling and hemodynamic monitoring. To determine radiotracer kinetics and biodistribution, sequential imaging was performed in closed-chest (n = 7) dogs under light anesthesia and physiological conditions with monitoring.

ACUTE MODEL. To determine the effects of regadenoson on coronary flow and myocardial radiotracer uptake, an open-chest canine preparation (n = 7) with a critical stenosis was used. A left lateral thoracotomy was performed and the heart suspended in a pericardial cradle. The proximal left anterior descending (LAD) and circumflex (LCX) arteries were dissected for placement of flow probes (Transonics Systems Inc., Ithaca, New York). A proximal critical LCX stenosis was created by the use of a hydraulic occluder and adjusted to blunt reactive hyperemia to a transient 10-s total coronary occlusion without impairing resting flow. Central temperature, HR, aortic pressure (AoP), and coronary flows were recorded. Radiolabeled microspheres (15-μm diameter; Sc-46, Nb-95, Ru-103, and Sn-113) were injected in the left atrium.

Protocol. CHRONIC STUDIES. Dogs had ^{201}Tl and ^{99m}Tc-MIBI vasodilator stress imaging performed on 2 successive weeks; week 1 with regadenoson and week 2 with adenosine. The week between studies is sufficient to ensure noninteraction between

ABBREVIATIONS AND ACRONYMS

AoP = aortic pressure
DPI = dynamic planar Imaging
HR = heart rate
IS = ischemic
LAD = left anterior descending artery
LCX = left circumflex artery
LV = left ventricular
MBF = myocardial blood flow
MPI = myocardial perfusion imaging
NI = nonischemic
%ID = percent injected dose
SPECT = single-photon emission computed tomography
^{99m}Tc = technetium-99m
^{201}Tl = thallium-201

sessions. During the first session (Fig. 1A), each dog received an intravenous injection of regadenoson (2.5 μg/kg) over 30 s and then ^{201}Tl (55.5 ± 7.4 MBq) 10 s later. Dynamic planar imaging (DPI; 15 min) followed the injection, along with timed arterial blood sampling for determination of radiotracer clearance kinetics by use of a roller-pump (20 samples at 15 s/sample, then 10 samples at 30 s/sample). Blood (0.5 ml) was collected, weighed, and counted in a gamma-well-counter. Two hours later, the same regadenoson vasodilator stress protocol was repeated with injection of ^{99m}Tc-MIBI (843.6 ± 148 MBq).

For the second session (Fig. 1B), the dogs received an intravenous infusion of adenosine at a rate of 280 μg/kg/min over 4.5 min. An injection of ^{201}Tl (59.2 ± 3.7 MBq) was given 1.5 min into the adenosine infusion. Then DPI and blood withdrawals, with use of the same protocol as with regadenoson, followed the injection. Two hours later, the adenosine stress protocol was repeated but with injection of ^{99m}Tc-MIBI (858.4 ± 144.3 MBq). The blood clearance half-time was calculated by the use of a logarithmic transform for both tracers with both vasodilators.

ACUTE STUDIES. On week 3, open-chest studies were performed (Fig. 1C) after creation of a critical LCX stenosis. Regadenoson (2.5 μg/kg) was injected intravenously over 30 s, and ^{201}Tl (51.8 ± 3.7 MBq), ^{99m}Tc-MIBI (873.2 ± 166.5 MBq), and radiolabeled microspheres were injected simultaneously 10 s after the regadenoson bolus. To minimize redistribution, dogs were euthanized 15 min after tracer injection. Regional myocardial flow was measured at rest and stress with radiolabeled microspheres by the use of established methods (2). Hearts were excised and cast with dental molding material (Alginate, Type I, fast-set, Quala Dental Products, ADC Milford, Delaware) for ex vivo single-photon emission computed tomography (SPECT) imaging, avoiding most of the confounding effects of attenuation and scatter. Hearts were sliced (5 mm), and each slice was divided into 8 radial pies. Segments underwent gamma-well-counting for the determination of tracer activity and microsphere flow.

Hemodynamics. Electrocardiogram, AoP, and coronary flows were recorded 30 s before and after infusion of the vasodilator (Sonolab, Sonometrics Inc., Ontario, Canada). R-waves were used to segment the signals into individual cardiac cycles. Heart rate, systolic and diastolic AoP, and peak LAD and LCX flow were determined every 10 s.

Planar imaging. Five-second images were acquired for the first 30 s followed by 30-s images for the

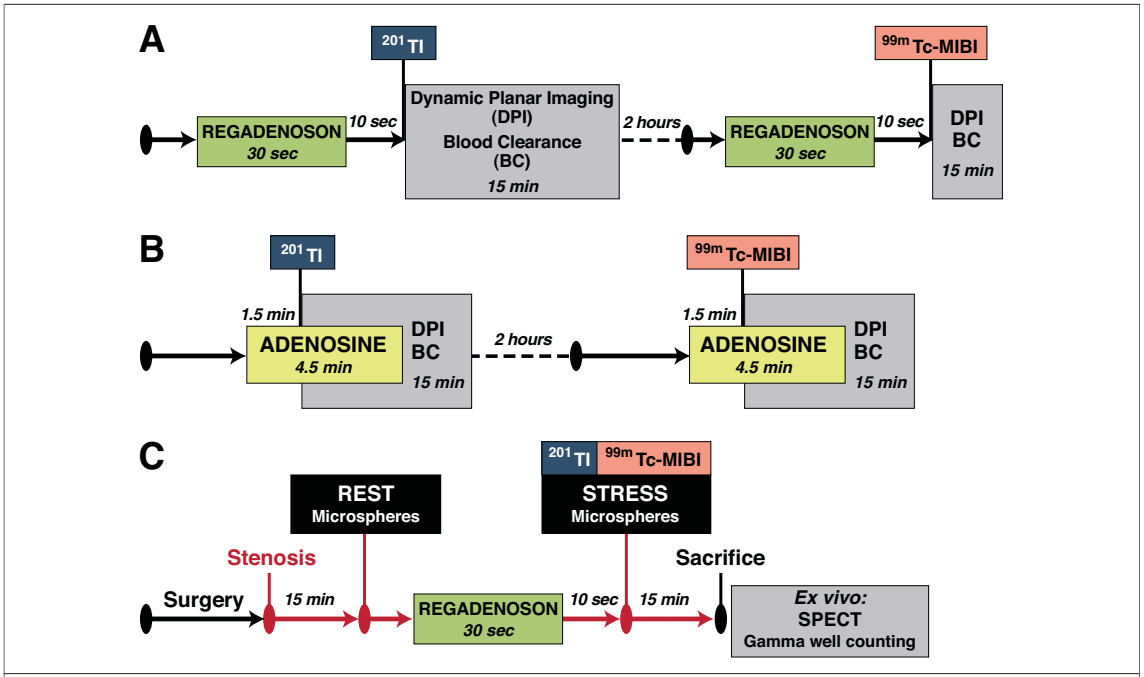

Figure 1. Experimental Protocols and Timelines

The protocol for closed-chest regadenoson studies performed on week 1 **(A)**, for closed-chest adenosine studies performed on week 2 **(B)**, and for an acute open-chest study performed on week 3 **(C)**. Hemodynamic acquisitions started 30 s before infusion of vasodilator. ^{99m}Tc = technetium-99m; ^{201}Tl = thallium-201.

Table 1. Hemodynamic Effects

Radiotracer	^{201}Tl		^{99m}Tc-MIBI	
Stressor	Adenosine	Regadenoson	Adenosine	Regadenoson
Peak values (% baseline)				
Diastolic AoP	76.6 ± 5.1*	70.5 ± 6.0*	75.5 ± 2.6*	75.7 ± 4.0*
Systolic AoP	84.9 ± 3.8*	81.7 ± 5.3*	83.2 ± 2.5*	85.1 ± 2.1*
Heart rate	131.3 ± 4.7*	122.2 ± 8.5*	123.3 ± 7.3*	120.7 ± 8.1*
2-min post-values (% baseline)				
Diastolic AoP	81.9 ± 4.5*†	77.5 ± 5.0*†	80.8 ± 2.1*†	80.1 ± 4.1*†
Systolic AoP	89.7 ± 3.3*†	87.7 ± 3.9*†	86.5 ± 2.2*†	89.2 ± 2.4*†
Heart rate	124.3 ± 4.5*†	113.5 ± 8.9†	117.8 ± 6.5*	116.1 ± 7.0*†
End values (% baseline)				
Diastolic AoP	97.5 ± 2.4	90.2 ± 4.8*	92.4 ± 3.7*	89.4 ± 1.3*
Systolic AoP	97.7 ± 2.9	89.2 ± 4.5*	93.6 ± 3.1*	92.0 ± 1.7*
Heart rate	103.1 ± 4.7	100.2 ± 6.4	97.0 ± 3.3	101.1 ± 5.7

Heart rate and systolic and diastolic AoP are shown for select time points after the stressor infusion. Shown are the peak alteration from baseline, the average change during the 2 min after radiotracer injection, and the value at 10 min after infusion of the stressor. There was no difference in the hemodynamic effects between groups. *$p < 0.05$ versus baseline. †$p < 0.05$ versus peak values.
AoP = aortic pressure; ^{99m}Tc = technetium-99m; ^{201}Tl = thallium-201.

remaining 14.5 min for analyzing changes in myocardial and background activity. Images were acquired with a large field-of-view gamma-camera (Millennium VG, GE Healthcare, Milwaukee, Wisconsin) by the use of a high-resolution, parallel-hole collimator. Images (256 × 256 matrix) were acquired without magnification in an anterior view by the use of appropriate energy windows for ^{201}Tl (71 ± 7.5% keV), and ^{99m}Tc-MIBI (140 ± 7.5% keV). Regions-of-interest were drawn over blood pool, myocardium, liver, lung, and kidney. Time-activity curves were generated for each organ, and activity was expressed as percent-injected dose/pixel (%ID/pixel) by the use of an external point source

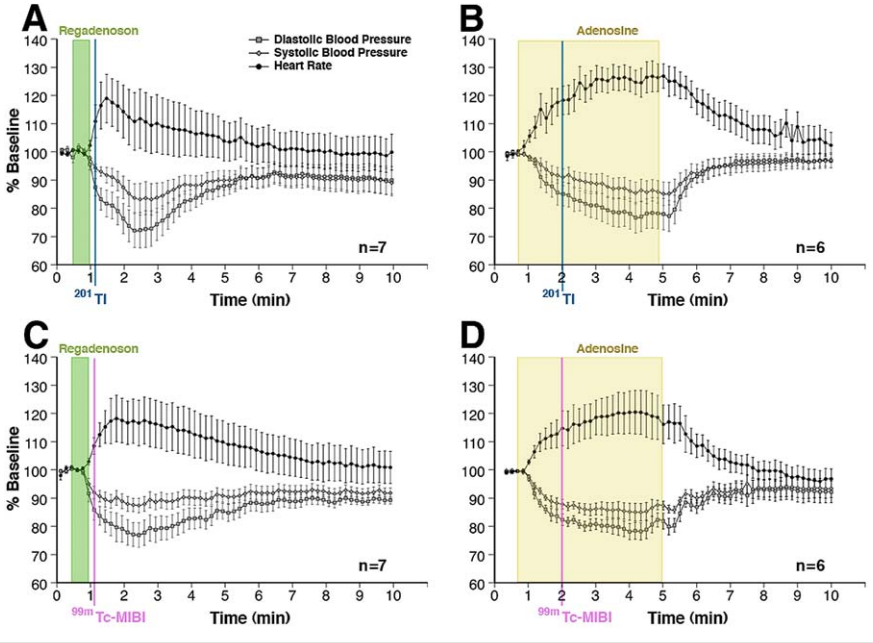

Figure 2. Hemodynamic Response in the Chronic Studies

Heart rate, systolic, and diastolic aortic pressure time-dependent changes (%baseline) after the stressor infusion (shaded box) for each isotope: **(A)** ^{201}Tl during regadenoson stress; **(B)** ^{201}Tl during adenosine stress; **(C)** ^{99m}Tc-MIBI during regadenoson stress; and **(D)** ^{99m}Tc-MIBI during adenosine stress. The **dashed line** indicates the radiotracer injection. The rapid effect of regadenoson is evident compared with the adenosine response. The hemodynamic effect for each stressor did not differ between isotope injections.

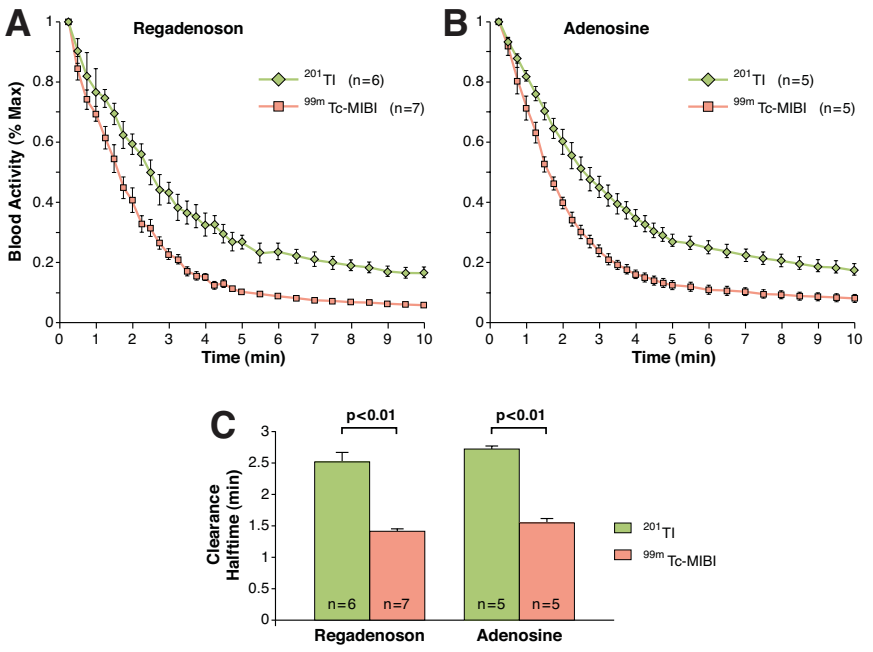

Figure 3. Clearance Half-Time and Biodistribution

The time-arterial blood activity curves for ^{201}Tl and ^{99m}Tc-MIBI after the infusion of regadenoson **(A)** or adenosine **(B)** are shown. **(C)** The clearance half-times for ^{201}Tl and ^{99m}Tc-MIBI with regadenoson and adenosine are shown. The clearance half-time is significantly shorter for ^{99m}Tc-MIBI than for ^{201}Tl with both stressors. **(D)** An example of a dynamic series of ^{99m}Tc-MIBI planar images, following a 30-s regadenoson infusion is shown. The images show where the regions-of-interest were drawn. The time-dependent biodistribution is shown as the logarithm (%ID/pixel) for ^{201}Tl and ^{99m}Tc-MIBI with both stressors **(E to H)**. The biodistribution at 15 min after injection was no different between stressors for ^{201}Tl and ^{99m}Tc-MIBI (**I** and **J**, respectively). *Continued on next page.*

of known activity. The myocardium-to-liver activity and myocardium-to-lung ratios, at 15 min for ^{201}Tl and ^{99m}Tc-MIBI, were compared.

Myocardial blood flow. Myocardial segments were weighed and counted within 24 h for determination of ^{201}Tl and ^{99m}Tc activity in a gamma-scintillation-counter (Packard Instruments, Milford, Connecticut) by the use of energy windows for ^{201}Tl, ^{99m}Tc, and all microspheres (^{201}Tl: 67 to 91 keV, ^{99m}Tc: 130 to 170 keV, ^{51}Cr: 290 to 360 keV, ^{113}Sn: 361 to 440 keV, ^{103}Ru: 460 to 550 keV, ^{95}Nb: 700 to 810 keV, ^{46}Sc: 811 to 1,160 keV). Samples were recounted 1 week after radiotracer injection to determine microsphere flow. Myocardial flow was calculated by the use of previously published methods, with correction for radiotracer decay, spill-up, and spill-down (2). Regional flow was expressed in ml/min/g, as well as a percent nonischemic and ischemic.

Ex vivo SPECT imaging. Ex vivo dual-isotope ^{201}Tl and ^{99m}Tc-MIBI SPECT imaging was performed by use of the same dual-head rotational gamma-camera, collimators, and energy windows applied for in vivo SPECT imaging. Images were acquired by the use of a 360° circular-orbit, in a step-and-shoot fashion (64 × 64 matrix; 5-mm slice thickness). No attenuation or scatter correction was required. Images were reconstructed by the use of filtered back-projection with ramp-filters. A 3-dimensional low-pass filter (Butterworth, order-4 and cutoff 0.35) was applied to post-reconstruction transverse SPECT slices, and images were reoriented into cardiac-specific axes.

The Yale-CQ-algorithm was used to quantify the SPECT images (19,20). Circumferential count profiles were generated for a series of left ventricular (LV) short-axis images. Three anatomic slices were divided into 128 radial sectors. Defects were defined as counts <80% of the maximum. ^{201}Tl and ^{99m}Tc-MIBI integrated defect scores (%LV) were calculated, providing an index of both the magnitude and extent of the perfusion abnormality.

Statistical analysis. Ischemic (IS) and nonischemic (NI) segments were defined by a coronary flow reserve <1.5 and >2.5, respectively. On the basis of this myocardial segmentation, IS/NI tracer and flow ratios were calculated and compared. All values are expressed as mean ± SEM. Statistical differences of the physiologic, hemodynamic, and radiolabeled

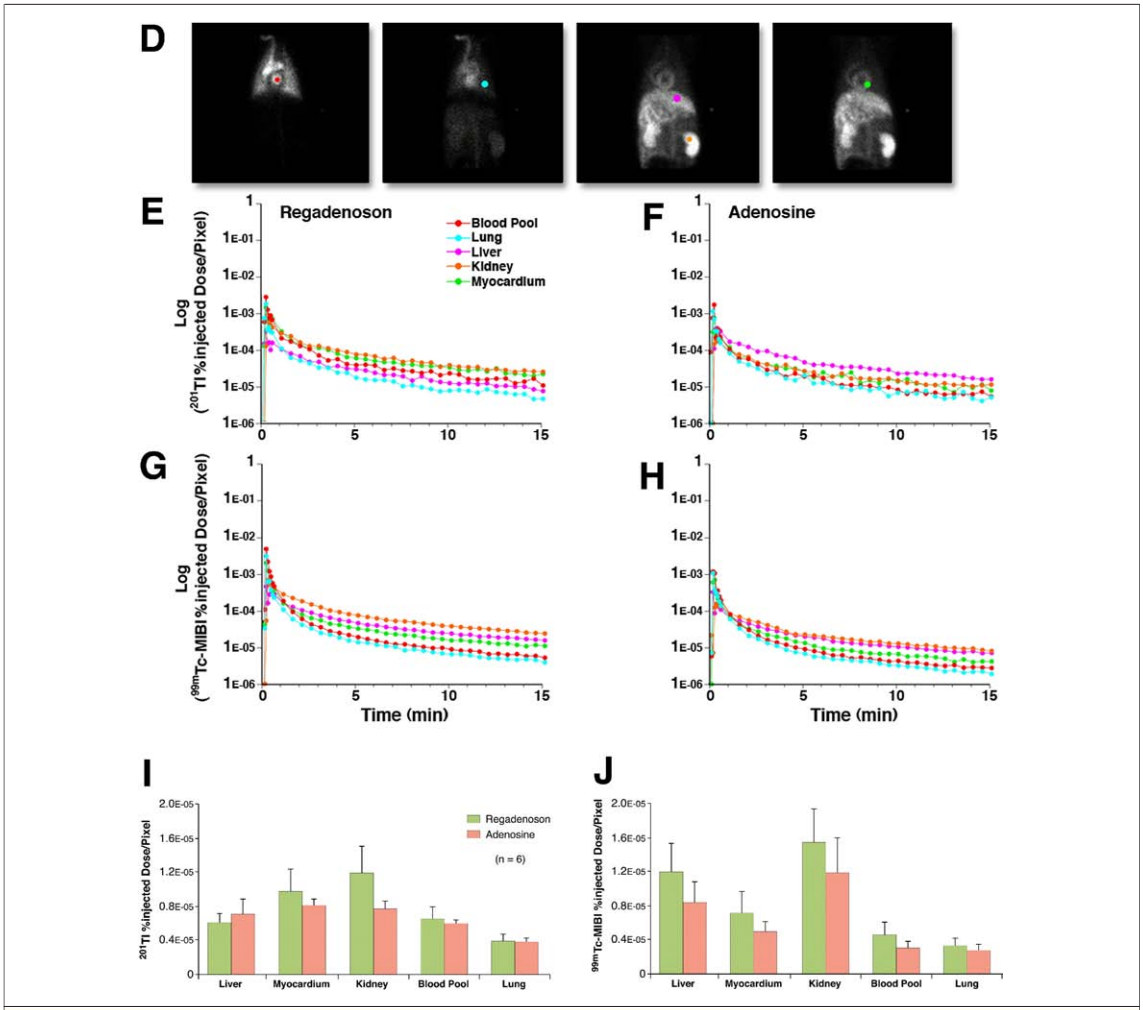

Figure 3. Continued.

tracer between the regadenoson- and adenosine-treated animals were assessed using a one-way analysis of variance. For conditions that demonstrated a significant main effect, post-hoc analyses were performed with either a *t* test (comparison between 2 populations) or a *z* test (comparison with %baseline).

RESULTS

Chronic studies. HEMODYNAMICS. A 30-s bolus of regadenoson and a 4.5-min infusion of adenosine produced similar hemodynamic effects (p = NS) (Table 1). Peak HR significantly increased ($p < 0.05$), and peak systolic and diastolic AoP significantly decreased ($p < 0.05$) relative to baseline values. These parameters were significantly ($p < 0.05$) different than baseline 2 min after injection of the radiotracers. These values tended to return to baseline within 10 min (Fig. 2). The peak effect of regadenoson occurs ~30 s after the bolus, whereas the peak effect of adenosine occurs 1.5 to 2 min after beginning the infusion, corresponding to radiotracer injection. The duration of the peak hemodynamic effect was shorter for regadenoson than for adenosine, although sufficient to create differential uptake of ^{201}Tl and ^{99m}Tc-MIBI.

RADIOTRACER CLEARANCE AND BIODISTRIBUTION. The arterial blood clearance half-time was significantly faster ($p < 0.01$) for ^{99m}Tc-MIBI (regadenoson: 1.4 ± 0.03 min; adenosine: 1.5 ± 0.08 min) than for ^{201}Tl (regadenoson: 2.5 ± 0.16 min; adenosine: 2.7 ± 0.04 min) (Figs. 3A to 3C).

There was no statistical difference in the biodistribution of ^{201}Tl or ^{99m}Tc-MIBI associated with regadenoson and adenosine. However, ^{201}Tl (regadenoson: 1.63 ± 0.31; adenosine: 1.37 ± 0.20) had significantly greater ($p < 0.05$) myocardium-to-liver ratios compared with ^{99m}Tc-MIBI (regadeno-

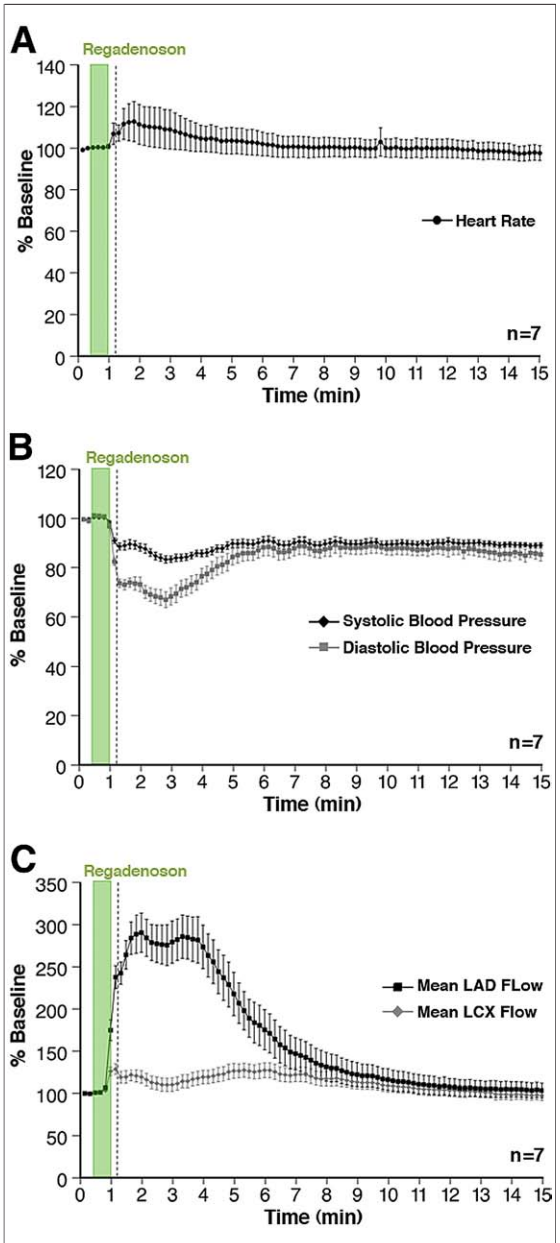

Figure 4. Hemodynamic Response in Acute Studies

The hemodynamic response to the 30-s regadenoson bolus **(shaded box)** for the acute studies: heart rate **(A)**, systolic and diastolic aortic pressure response **(B)**, and LAD and LCX coronary flow **(C)** responses. All values are %baseline. The **dashed line** indicates the radiotracer injection. There was a 3-fold increase in nonstenotic LAD flow and no increase in LCX flow. LAD = left anterior descending; LCX = left circumflex artery.

son: 0.56 ± 0.06; adenosine: 0.60 ± 0.06) at 15 min after injection. There was no difference in the myocardium-to-lung ratio between ^{201}Tl (regadenoson: 2.84 ± 0.64; adenosine: 2.36 ± 0.47) and ^{99m}Tc-MIBI (regadenoson: 2.12 ± 0.18; adenosine: 1.82 ± 0.09) at 15 min after injection. The radiotracer uptake during the initial 15 min after injection also was expressed as a %ID/pixel (Figs. 3D to 3J).

Acute studies. HEMODYNAMICS. In the acute studies (n = 7), the 30-s bolus of regadenoson caused a nearly significant increase in HR ($p < 0.08$) and a decrease ($p < 0.05$) in both systolic and diastolic AoP during the 2-min post-radiotracer injection, similar to the chronic studies. The pressures remained mildly reduced (~10 mm Hg; $p < 0.05$) at 10 min after regadenoson administration. The flow in the stenotic LCX increased on average 6.7% ($p < 0.05$) over baseline, which is consistent with ablation of reactive hyperemia. In the LAD, however, the flow significantly increased (2.5- to 3-fold baseline; $p < 0.001$) during the 2 min after radiotracer injection. The LAD flow returned to baseline values at 10 min after regadenoson infusion (Fig. 4).

MYOCARDIAL MICROSPHERE BLOOD FLOW. Transmural myocardial microsphere blood flow (Fig. 5) was similar between IS (0.86 ± 0.24 ml/min/g) and NI (0.89 ± 0.26 ml/min/g) territories at baseline. Regadenoson caused ~3.3-fold increase in myocardial blood flow (MBF) in the NI territory (2.98 ± 0.98 ml/min/g; $p < 0.05$), whereas MBF in the ischemic territory was unchanged (0.95 ± 0.23 ml/min/g, p = NS).

MYOCARDIAL RADIOTRACER ACTIVITY VERSUS FLOW. The deficit in relative myocardial uptake of ^{201}Tl and ^{99m}Tc-MIBI in the stenotic region during regadenoson vasodilator stress underestimated the relative microsphere blood flow deficit. The

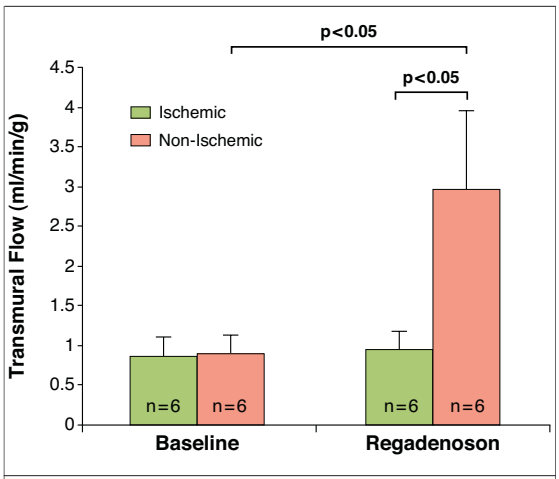

Figure 5. Transmural Absolute Myocardial Blood Flow

Average microsphere flows for ischemic and nonischemic regions at rest and during vasodilator stress. The blood flows are comparable at rest in both regions. Flows during regadenoson vasodilator stress increased 3-fold in the nonischemic region but remained unchanged in the ischemic region with a critical stenosis.

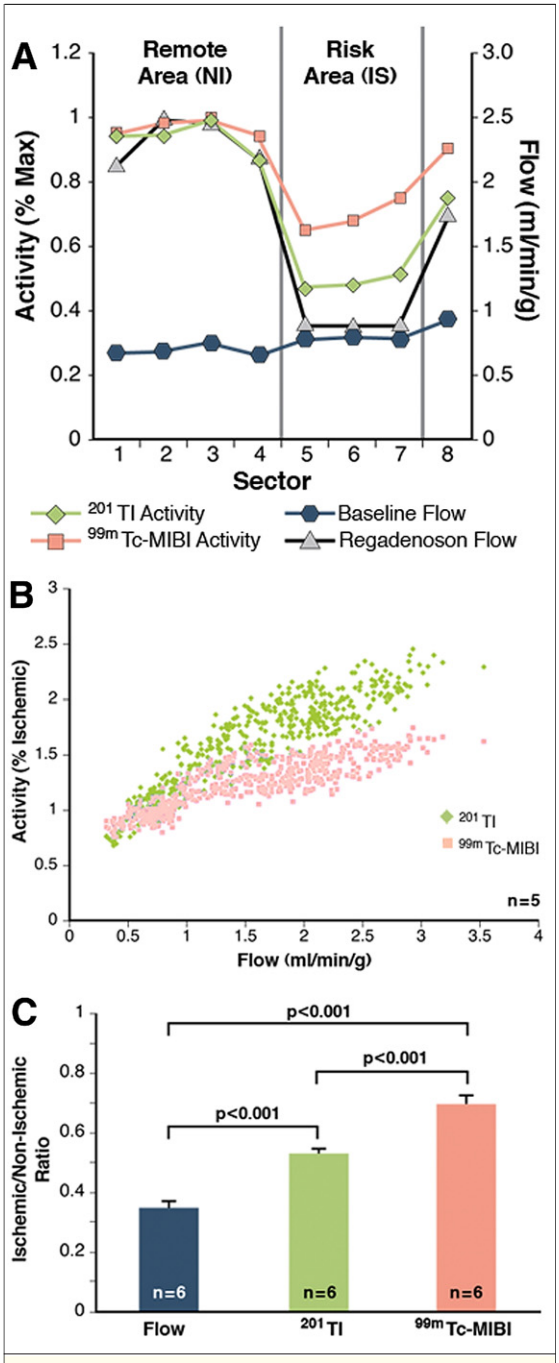

Figure 6. Perfusion Deficit

(A) Circumferential profile from a representative left ventricular short-axis slice is shown. There was uniform flow at rest and a significant heterogeneity of flow with regadenoson as measured by microspheres. **(B)** Tracer activity (%Ischemic) versus flow is shown. Regional myocardial ^{99m}Tc-MIBI activity plateaus at greater flows. **(C)** The ischemic/nonischemic ratio for flow, ^{201}Tl, and ^{99m}Tc-MIBI is shown. Both radiotracers significantly underestimate flow heterogeneity. IS = ischemic; NI = nonischemic; other abbreviations as in Figure 1.

spatial variation of radiotracer uptake and myocardial microsphere flow is shown for a representative myocardial short-axis slice (Fig. 6A). Relative ^{201}Tl activity approximated the flow deficit within the ischemic region better than ^{99m}Tc-MIBI activity. Figure 6B shows the relationship between absolute myocardial flow and relative ^{201}Tl and ^{99m}Tc-MIBI retention for all segments of 1 dog. There was a linear relationship between relative myocardial ^{201}Tl activity and microsphere flow, even at the high flows achieved with regadenoson. However, there was considerable "roll-off" of ^{99m}Tc-MIBI at flows ~1.5 times above resting flow (Fig. 6B). The myocardial IS/NI ratio of both ^{201}Tl (0.53 ± 0.02) and ^{99m}Tc-MIBI (0.69 ± 0.03) significantly underestimated ($p < 0.001$) the true flow deficit (0.34 ± 0.02). However, the underestimation associated with ^{201}Tl activity was significantly ($p < 0.001$) less than that observed for ^{99m}Tc-MIBI (Fig. 6C).

EX VIVO SPECT QUANTIFICATION. The differences in relative regional ^{201}Tl and ^{99m}Tc-MIBI uptake within the stenotic territory during regadenoson stress, demonstrated by gamma-well-counting, could also be visualized on ex vivo SPECT imaging, under conditions of minimal attenuation and scatter. Ex vivo images clearly showed the perfusion heterogeneity created using regadenoson in the presence of a critical stenosis (Fig. 7A). However, the perfusion defect appears larger and more noticeable with ^{201}Tl compared with ^{99m}Tc-MIBI, despite the lower count density. The integrated perfusion defect score was significantly

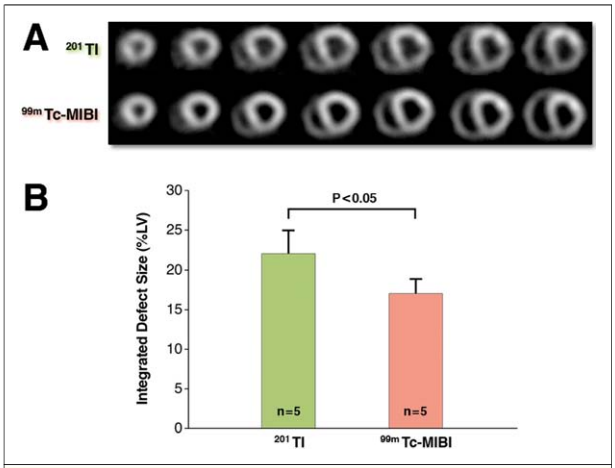

Figure 7. SPECT Integrated Defect Size

(A) Series of ^{201}Tl and ^{99m}Tc-MIBI ex vivo short-axis slices from a representative dog are shown. With a critical stenosis, there were no marked perfusion defects; however, the perfusion defects were visually smaller in ^{99m}Tc-MIBI images compared with ^{201}Tl images. **(B)** The integrated defect magnitude calculated using the Yale-CQ-quantitative-program is shown. %LV = percent left ventricular; other abbreviations as in Figure 1.

larger ($p < 0.05$) with ^{201}Tl (22 ± 2.8 %LV) than with ^{99m}Tc-MIBI (17 ± 1.7 %LV) (Fig. 7B).

DISCUSSION

The current study compared the effects of regadenoson and adenosine on systemic hemodynamics, radiotracer biodistribution, and clearance kinetics in clinically relevant canine models to define the optimal approach for MPI by the use of vasodilator stress. A regadenoson bolus (2.5 μg/kg) produced systemic hemodynamic effects similar to a 4.5-min adenosine infusion. Regadenoson created a 2.5- to 3-fold augmentation in microspheres flow. The HR, AoP, and coronary flow remained altered during the critical 2-min post-radiotracer injection. These effects on flow were comparable to those observed by Lieu et al. (18) in human studies, in which they used a Doppler flow wire measuring the coronary flow velocity in response to a 400-μg or 500-μg bolus of regadenoson. These doses were greater than what was administered to the dogs in the current study after body mass correction.

Although regadenoson and adenosine are known to have differential effects on renal and splanchnic flow (10), both vasodilators caused a similar biodistribution and clearance of ^{201}Tl and ^{99m}Tc-MIBI. The use of DPI demonstrated a favorable biodistribution of both radiotracers, which was comparable between the vasodilators. Unexpectedly, we observed a faster blood clearance of ^{99m}Tc-MIBI (1.5 min) compared with ^{201}Tl (2.5 min) with both vasodilators. This finding suggests that a longer duration of vasodilator stress, regardless of the specific vasodilator, might be more important after injection of ^{201}Tl than after injection of ^{99m}Tc-MIBI. However, ^{201}Tl performed better as a perfusion agent for the detection of relative flow heterogeneity using regadenoson as defined by ex vivo SPECT and well-counting techniques.

The injection of ^{201}Tl or ^{99m}Tc-MIBI 10 s after the 30-s bolus of regadenoson provided high-quality ex vivo SPECT images, demonstrating significant heterogeneity of relative myocardial perfusion in the presence of a critical stenosis. These ex vivo images were acquired under ideal imaging conditions with minimal attenuation and scatter. On the basis of tissue counting, both ^{201}Tl and ^{99m}Tc-MIBI underestimated the true MBF heterogeneity as measured using microspheres. This finding is consistent with previous studies in which the authors evaluated ^{201}Tl and ^{99m}Tc-MIBI MPI during adenosine stress (9) and other selective A_{2A} adenosine agonists (21). We observed the expected plateau of radiotracer uptake at higher flows, which has been attributed to a diffusion limitation of radiotracer uptake. In the case of ^{201}Tl, some of the flow underestimation may be attributed to differential washout of ^{201}Tl from the normal and ischemic regions, since the radiotracer distribution was evaluated at 15 min after radiotracer injection. Therefore, there may have been a slight component of ^{201}Tl redistribution contributing to the observed plateau of ^{201}Tl retention. Despite the potential for early ^{201}Tl redistribution, the more linear myocardial uptake of ^{201}Tl relative to flow during vasodilator stress with regadenoson suggests that ^{201}Tl may be better than ^{99m}Tc-MIBI or other similar ^{99m}Tc-labeled perfusion agents for use with vasodilator stress.

Although in this study a matched group of acute studies was not performed with adenosine, Glover et al. (9) previously reported similar results using adenosine in an open-chest canine study. Glover et al. (9) evaluated ^{201}Tl and ^{99m}Tc-MIBI uptake relative to microsphere flow in the presence of 2 levels of stenosis. Their creation of a "critical stenosis" was designed to ablate reactive hyperemia, similar to our acute studies. The microsphere flows in both studies demonstrated no increase in flow in the stenotic territory and ~3.5-fold flow increase in the remote territory in response to vasodilator stress. Glover et al. (9) used planar imaging of excised LV slices from dogs euthanized 5 min after injection of radiotracers compared with ex vivo SPECT imaging in our study. They demonstrated a similar underestimation of the true flow deficit (0.17 ± 0.03) with both ^{201}Tl (0.37 ± 0.05) and ^{99m}Tc-MIBI (0.53 ± 0.06) and that ^{201}Tl provided a better estimation of the flow deficit (9), similar to our observation using regadenoson.

The recent ADVANCE (ADenoscan Versus regAdenosoN Comparative Evaluation for Myocardial Perfusion Imaging) phae 3 multicenter international trial showed no difference between regadenoson and adenosine for determination of reversible perfusion defects with ^{99m}Tc-MIBI or ^{99m}Tc-Tetrofosmin, although the chi-squares for both the adenosine-regadenoson and adenosine-adenosine comparisons were only 0.63 or 0.64, respectively, suggesting only a fair concordance (14). On the basis of our experimental findings, ^{201}Tl may offer a clinical advantage over the ^{99m}Tc-labeled perfusion agents and improve test reproducibility for determination of the extent of ischemia. Importantly, the current finding regarding the biodistribution and ex vivo SPECT imaging would predict that there should be no significant clini-

cal difference between regadenoson and adenosine for MPI.

Although this pre-clinical study provides important insight regarding regadenoson and adenosine stress MPI, these studies were performed during anesthesia, which could produce confounding effects on systemic hemodynamics. In clinical studies (13,14), the hemodynamic changes associated with regadenoson were less and shorter-lasting than those observed in our study. Our study was specifically performed with the use of the volatile anesthetic halothane. Because Hickey et al. (22) found that there was no significant change in coronary flow reserve between conscious and halothane-anesthetized canines.

In addition, to minimize any potential adverse effect, the chronic studies were performed with the use of a closed-chest preparation that required very light anesthesia with halothane and nitrous oxide. Although halothane is a mild cardiac depressant, the effects are dose dependent (23,24). Therefore, the light plane of anesthesia used should have had little effect on cardiac output and the biodistribution of the radiotracers. Our hemodynamic results on anesthetized dogs closely matched the result from previous studies on conscious dogs (11) and were within physiological ranges throughout the study protocol. Glover et al. (9) used sodium pentobarbital anesthesia in their study and showed very similar hemodynamic responses to adenosine and similar kinetic behavior of ^{201}Tl and ^{99m}Tc-MIBI during adenosine stress (9).

Our anesthetized preparation offers advantages over clinical studies or conscious preparations, enabling serial imaging without risk of any subject movement, which is a significant confounder in clinical studies with repeated imaging. The changes in flow that we observed in our experimental model during vasodilator stress are concordant with a clinical study (25) in which the authors used rest and adenosine oxygen-15 water positron emission tomographic imaging in control subjects. Coronary vasodilator reserve (3.16 ± 1.4) in control patients during adenosine stress was nearly identical to the ~3.3-fold increase we obtained in the NI territory in response to regadenoson vasodilator stress.

CONCLUSIONS

The bolus administration of regadenoson produced a hyperemic response comparable to a standard infusion of adenosine. The biodistribution and clearance kinetics of both ^{201}Tl and ^{99m}Tc-MIBI during regadenoson were similar to adenosine vasodilation. Ex vivo perfusion images under the most ideal conditions permitted detection of a critical stenosis, although ^{201}Tl offered significant advantages over ^{99m}Tc-MIBI for perfusion imaging during regadenoson vasodilator stress.

Acknowledgments

The authors acknowledge the technical assistance of Xiao-Yu Hu, Brian Bourke, Carol Akirav, Lori Brown, and Stacy Sullivan.

Reprint requests and correspondence: Dr. Albert J. Sinusas, Yale University School of Medicine, Nuclear Cardiology, 3FMP, P.O. Box 208017, New Haven, Connecticut 06520-8017. *E-mail: albert.sinusas@yale.edu.*

REFERENCES

1. Canby RC, Silber S, Pohost GM. Relations of the myocardial imaging agents 99mTc-MIBI and 201T1 to myocardial blood flow in a canine model of myocardial ischemic insult. Circulation 1990;81:289–96.
2. Sinusas AJ, Watson DD, Cannon JM, Jr., Beller GA. Effect of ischemia and postischemic dysfunction on myocardial uptake of technetium-99m-labeled methoxyisobutyl isonitrile and thallium-201. J Am Coll Cardiol 1989;14:1785–93.
3. Wackers FJ, Berman DS, Maddahi J, et al. Technetium-99m hexakis 2-methoxyisobutyl isonitrile: human biodistribution, dosimetry, safety, and preliminary comparison to thallium-201 for myocardial perfusion imaging. J Nucl Med 1989;30:301–11.
4. Calnon DA, Glover DK, Beller GA, et al. Effects of dobutamine stress on myocardial blood flow, 99mTc sestamibi uptake, and systolic wall thickening in the presence of coronary artery stenoses: implications for dobutamine stress testing. Circulation 1997;96:2353–60.
5. Candell-Riera J, Santana-Boado C, Castell-Conesa J, et al. Simultaneous dipyridamole/maximal subjective exercise with 99mTc-MIBI SPECT: improved diagnostic yield in coronary artery disease. J Am Coll Cardiol 1997;29:531–6.
6. Cramer MJ, Verzijlbergen JF, Van der Wall EE, et al. Head-to-head comparison between technetium-99m-sestamibi and thallium-201 tomographic imaging for the detection of coronary artery disease using combined dipyridamole-exercise stress. Coron Artery Dis 1994;5:787–91.
7. Marwick T, Willemart B, D'Hondt AM, et al. Selection of the optimal nonexercise stress for the evaluation of ischemic regional myocardial dysfunction and malperfusion. Comparison of dobutamine and adenosine using echocardiography and 99mTc-MIBI single photon emission computed tomography. Circulation 1993;87:345–54.
8. Santos-Ocampo CD, Herman SD, Travin MI, et al. Comparison of exercise, dipyridamole, and adenosine by use of technetium 99m sestamibi tomographic imaging. J Nucl Cardiol 1994;1:57–64.
9. Glover DK, Ruiz M, Edwards NC, et al. Comparison between 201Tl and 99mTc sestamibi uptake during adenosine-induced vasodilation as a function of coronary stenosis severity. Circulation 1995;91:813–20.

10. Zhao G, Linke A, Xu X, et al. Comparative profile of vasodilation by CVT-3146, a novel A2A receptor agonist, and adenosine in conscious dogs. J Pharmacol Exp Ther 2003;307:182–9.
11. Trochu JN, Zhao G, Post H, et al. Selective A2A adenosine receptor agonist as a coronary vasodilator in conscious dogs: potential for use in myocardial perfusion imaging. J Cardiovasc Pharmacol 2003;41:132–9.
12. Cerqueira MD, Nguyen P, Staehr P, Underwood SR, Iskandrian AE. Effects of age, gender, obesity, and diabetes on the efficacy and safety of the selective A2A agonist regadenoson versus adenosine in myocardial perfusion imaging integrated ADVANCE-MPI trial results. J Am Coll Cardiol Img 2008;1:307–16.
13. Hendel RC, Bateman TM, Cerqueira MD, et al. Initial clinical experience with regadenoson, a novel selective A2A agonist for pharmacologic stress single-photon emission computed tomography myocardial perfusion imaging. J Am Coll Cardiol 2005;46: 2069–75.
14. Iskandrian AE, Bateman TM, Belardinelli L, et al. Adenosine versus regadenoson comparative evaluation in myocardial perfusion imaging: results of the ADVANCE phase 3 multicenter international trial. J Nucl Cardiol 2007;14:645–58.
15. Leaker BR, O'Connor B, Hansel TT, et al. Safety of regadenoson, an adenosine A2A receptor agonist for myocardial perfusion imaging, in mild asthma and moderate asthma patients: a randomized, double-blind, placebo-controlled trial. J Nucl Cardiol 2008;15: 329–36.
16. Thomas GS, Tammelin BR, Schiffman GL, et al. Safety of regadenoson, a selective adenosine A2A agonist, in patients with chronic obstructive pulmonary disease: A randomized, double-blind, placebo-controlled trial (RegCOPD trial). J Nucl Cardiol 2008;15:319–28.
17. Gao Z, Li Z, Baker SP, et al. Novel short-acting A2A adenosine receptor agonists for coronary vasodilation: inverse relationship between affinity and duration of action of A2A agonists. J Pharmacol Exp Ther 2001;298: 209–18.
18. Lieu HD, Shryock JC, von Mering GO, et al. Regadenoson, a selective A2A adenosine receptor agonist, causes dose-dependent increases in coronary blood flow velocity in humans. J Nucl Cardiol 2007;14:514–20.
19. Liu YH, Sinusas AJ, DeMan P, Zaret BL, Wackers FJ. Quantification of SPECT myocardial perfusion images: methodology and validation of the Yale-CQ method. J Nucl Cardiol 1999;6:190–204.
20. Liu YH, Sinusas AJ, Shi CQ, et al. Quantification of technetium 99m-labeled sestamibi single-photon emission computed tomography based on mean counts improves accuracy for assessment of relative regional myocardial blood flow: experimental validation in a canine model. J Nucl Cardiol 1996; 3:312–20.
21. Glover DK, Ruiz M, Takehana K, et al. Pharmacological stress myocardial perfusion imaging with the potent and selective A(2A) adenosine receptor agonists ATL193 and ATL146e administered by either intravenous infusion or bolus injection. Circulation 2001;104: 1181–7.
22. Hickey RF, Sybert PE, Verrier ED, Cason BA. Effects of halothane, enflurane, and isoflurane on coronary blood flow autoregulation and coronary vascular reserve in the canine heart. Anesthesiology 1988;68:21–30.
23. Bahlman SH, Eger EI, II, Smith NT, et al. The cardiovascular effects of nitrous oxide-halothane anesthesia in man. Anesthesiology 1971;35:274–85.
24. Vatner SF, Smith NT. Effects of halothane on left ventricular function and distribution of regional blood flow in dogs and primates. Circ Res 1974;34: 155–67.
25. Uren NG, Melin JA, De Bruyne B, Wijns W, Baudhuin T, Camici PG. Relation between myocardial blood flow and the severity of coronary-artery stenosis. N Engl J Med 1994; 330:1782–8.

Key Words: regadenoson ■ myocardial perfusion imaging ■ adenosine ■ biodistribution ■ tracer kinetics.